# Fatigue crack propagation modeling in 2D structures using the CPCN-FEM node-based approach

*Mohammed* Bentahar[a], *Noureddine* Mahmoudi[b], *Nedir* Hachemi[c], *Youcef* Moulai Arbi[d]

[a] Universiy of Saida Dr. Moulay Tahar, Faculty of Technology, Department of Civil Engineering and Hydraulics, Saida, People's Democratic Republic of Algeria,
e-mail: bentahae@yahoo.fr, **corresponding author**,
ORCID ID: https://orcid.org/0000-0002-2166-678X

[b] University of Saida Dr. Moulay Tahar, Faculty of Technology, Department of Civil Engineering and Hydraulics, Saida, People's Democratic Republic of Algeria,
e-mail: mahmoudi.noureddine@yahoo.fr,
ORCID ID: https://orcid.org/0000-0002-9740-0857

[c] University of Mustapha Stambouli, Mascara, People's Democratic Republic of Algeria,
e-mail: nedirhachemidz@gmail.com,
ORCID ID: https://orcid.org/0009-0008-2211-0776

[d] University of Mustapha Stambouli, Laboratory of Quantum Physics of Matter and Mathematical Modeling (LPQ3M), Mascara, People's Democratic Republic of Algeria,
e-mail: youcef.moulaiarbi@univ-mascara.dz,
ORCID ID: https://orcid.org/0000-0002-6534-8820

https://doi.org/10.5937/vojtehg74-59257

FIELD: mechanical engineering, materials
ARTICLE TYPE: original scientific paper

*Abstract:*

*Introduction/purpose: The study aims to model fatigue-related crack propagation by introducing a numerical method, CPCN-FEM (Crack Propagation by Coordinates of Nodes – Finite Element Method), which predicts crack trajectories through the systematic generation of nodal coordinates around the crack front.*

*Methods: The approach defines four principal nodes to control the propagation direction and computes the stress intensity factors (K I) and (KII), along with the crack inclination angle (β). The method was implemented in FORTRAN to automate node tracking, coordinate updating, and stepwise crack advance in a two-dimensional elastic isotropic model. Simulations were conducted and compared with analytical crack-path solutions, using the Richard criterion to determine crack orientation.*

*Results: The numerical model reproduced expected crack trajectories with high agreement with analytical predictions and demonstrated stable displacement behavior across multiple propagation cases. Mesh integrity was preserved during all propagation steps, and no remeshing was required.*

*Conclusion: The findings show that CPCN-FEM provides an accurate, efficient, and mesh-preserving technique for modeling crack growth under fatigue, offering reliable predictions of crack path evolution in fracture mechanics.*

*Keywords: crack propagation, Stress Intensity Factor (SIF), finite element method, CPCN-FEM, node coordinates, fracture mechanics.*

## Introduction

Fracture mechanics is a relatively modern branch of solid mechanics, having seen its primary theoretical growth during the twentieth century. In parallel, the phenomenon of material fatigue attracted growing attention from researchers as early as the beginning of the 1900s. Both fields share a common objective: enabling engineers to anticipate the behavior of structures up to their eventual failure (Elguedj et al., 2006).

In this context, Kocańda et al. (2009) introduced a deterministic methodology to forecast fatigue crack growth in components subjected to variable-amplitude loading, including overload and underload cycles. More recently, Niu et al. (2023) investigated how the length of steel fibers affects fatigue crack propagation in ultra-high-performance concrete (UHPC) exposed to cyclic bending, employing both Paris' law and the J-integral, in addition to a theoretical model of multiple crack growth.

Other approaches, such as that proposed by Mehmet et al., focus on predicting fatigue life and crack propagation by incorporating cycle counting and stress ratio calculations. Ricardo et al. (2018) studied the influence of propagation speed on crack opening and closing stresses through finite element modeling of ASTM-type specimens. Ilie and Ince et al. (2022) developed a systematic 3D FEM-based model to simulate crack growth behavior.

Several innovative strategies for crack propagation analysis have also been introduced in recent literature. For example, Wysmulski et al. (2023) applied both numerical and experimental methods to analyze crack formation in a carbon-epoxy composite plate featuring a central hole. In a similar vein, Nie et al. (2025) proposed a fatigue-based model aimed at capturing the complexity of small-scale crack networks.

Borges et al. (2022) explored fatigue crack growth in aluminum alloy 2024-T351 using the plastic CTOD (Crack Tip Opening Displacement)

technique to examine strain rate effects. Complementarily, Robles et al. (2023) applied various evaluation methods to characterize crack progression in AA2024-T315, with a focus on improving data reliability.

Crusat et al. (2021) contributed a numerical model for crack propagation in two-dimensional semi-brittle structures using zero-thickness interface elements, integrated within a finite element framework and grounded in constitutive mechanics principles. Moreover, several researchers, including Zhang et al. (2023), Si et al. (2024), and Zhang et al. (2024) investigated crack nucleation processes in brittle materials through both experimental and numerical approaches.

Pramana et al. (2024) carried out a study combining experimental and computational analyses to understand crack propagation in Al 2024, with a focus on developing loading spectra based on the Paris equation. Numerous studies have also sought to determine and quantify stress intensity factors (SIFs). For example, Montasser et al. (2023) applied isometric analysis techniques for crack control, while Sadek et al. (2024) used both the J-integral and CTOD methods to calculate SIFs in various structural geometries.

Alshoaibi and Fageehi (2023) introduced the "split-knot" method in fracture simulations to enhance crack path prediction through successive linear segment growth. Bentahar et al. (2023) used the Extended Finite Element Method (XFEM) to analyze inclined cracks and to evaluate energy dissipation (ALLDMD) and deformation energy (ALLSE) during fatigue crack progression.

Furthermore, Sedmak et al. (2024) demonstrated the effectiveness of XFEM for simulating fatigue crack growth in welded joints, providing reliable estimates of cycles to failure. A complementary study by Sedmak et al. (2023) reinforced the value of XFEM for evaluating fatigue life through comprehensive case studies. In another development, Alshoaibi and Ariffin (2015) used a two-dimensional modeling approach to trace crack trajectories and evaluate the lifespan of structural components in the context of damage tolerance.

Finally, Rahman et al. (2024) examined crack development using finite element techniques, focusing on self-healing materials where fracture mechanics is coupled with oxidation kinetics.

The objective of the present work is to implement a novel computational approach, CPCN-FEM (Crack Propagation via Coordinates of Nodes – Finite Element Method), which allows for the accurate construction of four key nodes along the crack front. This framework enables not only the evaluation of stress intensity factors ($K_I$ and $K_{II}$), but also the calculation of the crack orientation angle β. The methodology is

applied to the crack propagation problem in an isotropic elastic material, enabling detailed modeling of the crack trajectory through a step-by-step numerical process.

## Fracture mechanics

### *Criterion of Richard 2D*

Richard's criterion, which is based on $K_V$, is superior to the toughness $K_{IC}$. Therefore, irregular crack growth occurs, as indicated by equation (1).

$$K_V = \frac{K_I}{2} + \frac{1}{2}\sqrt{K_I^2 + 5.366K_{II}^2} = K_{IC} \tag{1}$$

where $K_V$ is influenced by the stress intensity factors ($K_I$ and $K_{II}$).

The Richard criterion provides excellent approximations for the ultimate fracture surface, compared to the maximum tangential stress criterion by Erdogan and Sih (1963). Equation (2) allows determining the crack inclination angle (β):

$$\beta = \mp\left[140^\circ \frac{|K_{II}|}{|K_I| + |K_{II}|} - 70^\circ\left(\frac{|K_{II}|}{|K_I| + |K_{II}|}\right)^2\right] \tag{2}$$

where KI and KII are the stress intensity factors corresponding to Mode I and Mode II.

For $K_{II}$ greater than zero, angle β is less than zero and vice versa as long as $K_I$ remains above zero.

### *Nuismer's criterion*

The energy release rate indicator developed by Nuismer et al. (1975) is based on the assumption of a short-duration curved crack (Figure 1). Therefore, there are other parameters, such as the criterion by Amestoy et al. (1980) which relies on the energy release rate and depicts crack propagation in the context of 2D mixed-mode loading. The conclusions for the crack deflection angles and the fracture limit curve correspond to those of the maximum tangential stress criterion (Richard et al, 2004). Bilby and Cardew (1975) address this criterion.

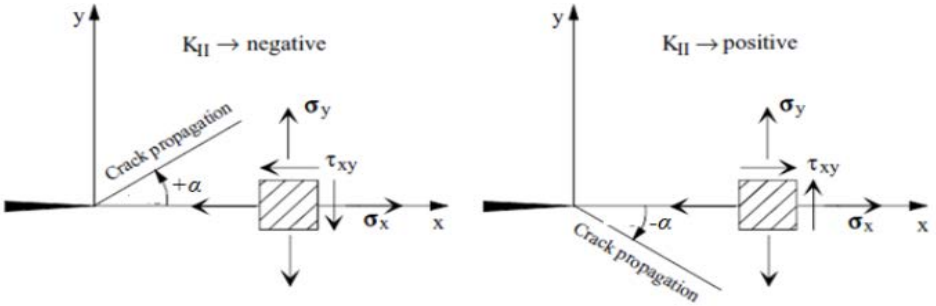


*Figure 1 - Illustration of crack propagation using Richard's criterion [31]*

## *Stress field*

For the coordinates r and θ, Tada et al. (2000) provided the equation of the two-dimensional stress field close to the fracture tip, which is described by the stress intensity factor K.

$$\sigma_{i,j}^{I,II}(r,\theta) = \frac{K_{I,II}}{\sqrt{2\pi r}} f(\theta) \tag{3}$$

$K_{I,\,II}$ is the SIF in Mode I and II,

$\sigma_{i,j}^{I,II}$ is the stress field associated with Mode I and II.

Consequently, singular elements must be constructed to precisely characterize the singularity field at the crack front. Since the leading front method generates triangular elements from boundary faces, the area surrounding the crack front must be separated before generating singular elements (Zienkiewicz et al, 2005). First, nodes are created around the crack tip in a rosette manner, then the node at the crack front and the associated edge segments are extracted. The rosette elements are then constructed by forming triangles as shown in Figure 2.

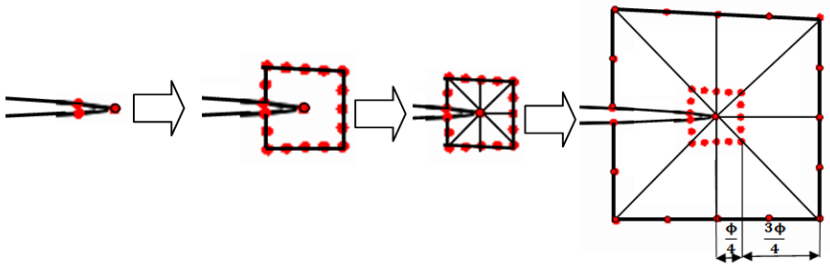


*Figure 2 - Special finite elements quarter point around the crack front*

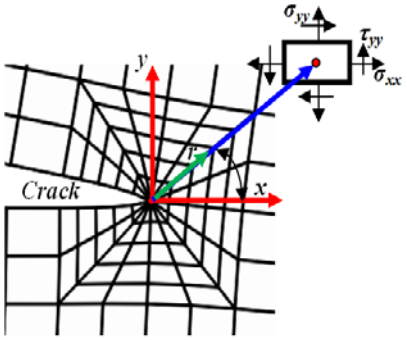


*Figure 3 - Stress field around the crack front*

$$\sigma_{xx} = \frac{K_I}{\sqrt{2\pi r}}\cos\frac{\theta}{2}\left(1-\sin\frac{\theta}{2}\sin\frac{3\theta}{2}\right)$$
$$\sigma_{yy} = \frac{K_I}{\sqrt{2\pi r}}\cos\frac{\theta}{2}\left(1+\sin\frac{\theta}{2}\sin\frac{3\theta}{2}\right) \quad (4)$$
$$\tau_{xy} = \frac{K_I}{\sqrt{2\pi r}}\sin\frac{\theta}{2}\cos\frac{\theta}{2}\cos\frac{3\theta}{2}$$

### *Stress Intensity Factor*

Saverio et al. (2024) defined the stress intensity factor K as a parameter which makes it possible to determine the state of stress and strain at any point in the vicinity of the crack.

$$K_I = R\sigma\sqrt{a\pi} \quad (5)$$

where R is the geometric correction factor of the model used.

$$R = 1.12 - 0.23\left(\frac{a}{L}\right) + 10.6\left(\frac{a}{L}\right)^2$$
$$-21.7\left(\frac{a}{L}\right)^3 + 30.4\left(\frac{a}{L}\right)^4$$

where $a$ is the crack length [mm] and $L$ is the length of the structure.

The stress intensity factor KII is given by the relation

$$K_I \sin\theta + K_{II}(3\sin\theta - 1) = 0 \qquad (7)$$

## Numerical model

We consider an elastic material structure of isotropic behavior, as shown in Figure 4. The structure has a height B = 20 mm and a length L = 18 mm, and 4 node elements were used in this analysis. The structure is subjected to a tensile stress applied to the upper surface of σ = 110 MPa, and the lower part is subjected to a fixed boundary condition. The mechanical properties of the material (Aluminum Alloy, AA) are E = 72,400 MPa and Poisson's ratio *v* is 0.3.

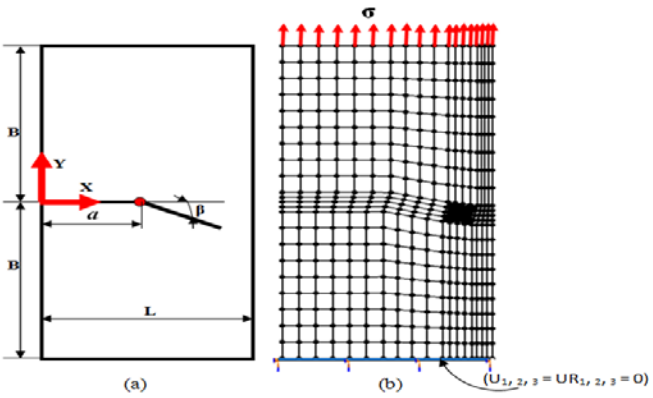


*Figure 4 - CPCN-FEM model*

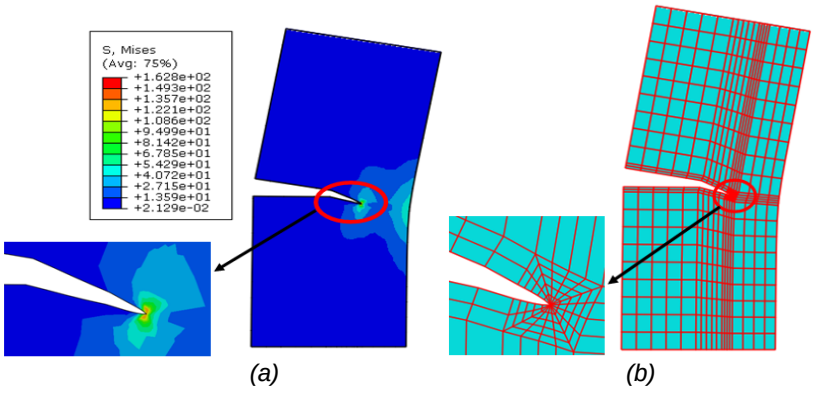


*Figure 5 - a) stress field and b) crack propagation on the CPCN-FEM model*

Figure 5 illustrates the crack propagation trajectory for different crack inclination angles using the CPCN-FEM approach. Furthermore, Figure 5a

illustrates the stress field in the vicinity of the crack front, and Figure 5b shows the different contours around the crack front.

## Strategy of the CPCN-FEM method

Creation of node coordinates by the Finite Element Method (CPCN-FEM) at the crack front of each crack propagation stage comprises the following steps:

Creation of the node coordinates for the first propagation, Fig. 6a;
Creation of the node coordinates for the second propagation, Fig. 6b;
Creation of the node coordinates for the third propagation Fig. 6c;
Creation of the node coordinates for the fourth propagation Fig. 6d;
Creation of the node coordinates for the fifth propagation Fig. 6e;
Creation of the node coordinates for the sixth propagation Fig. 6f.

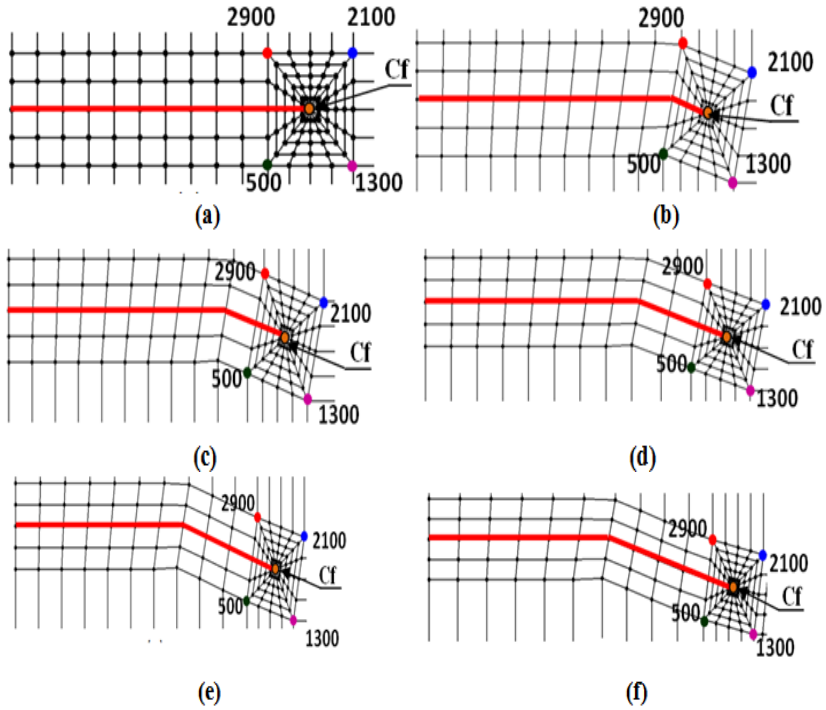


*Figure 6 - Strategy of the CPCN-FEM method: a) 1st propagation, b) 2nd propagation, c) 3rd propagation, d) 4th propagation, e) 5th propagation and f) 6th propagation*

## *Coordinates of the nodes*

### *Initial crack*

*Table 1 - Coordinates of the nodes on the initial crack front*

| Nodes | Coordinates | |
|---|---|---|
| | X | Y |
| 2900 | a -ϕ/2 | +ϕ /2 |
| 2100 | a +ϕ /2 | +ϕ /2 |
| 1300 | a -ϕ /2 | -ϕ /2 |
| 500 | a +ϕ /2 | -ϕ /2 |

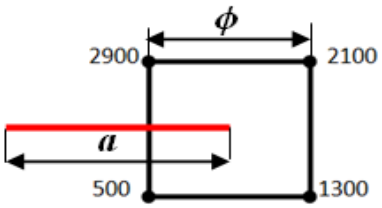


*Figure 7 - Initial crack with length a with node numbering*

The coordinates of the four nodes for the initial crack are given by equation (8):

$$X_i = a - S\frac{\phi}{2}$$
$$Y_i = S\frac{\phi}{2} \quad (8)$$

where i=2900, 2100,1300 and 500 with S=1 for the X coordinate of 2900 and 500 and the Y coordinate of 2900 and 2100, and S= -1, for the X coordinate of 2100 and 1300 and the Y coordinate of 500 and 1300. Moreover, a is the crack length [mm], measured from the centerline of the structure, ϕ is the total crack front length [mm], i.e., the span of the crack opening in the Y-direction at the crack front, and S is a directional scaling factor used to distribute the nodes symmetrically around the crack front. Its values are S=±1, depending on the node location, to simplify the expressions for X and Y coordinates in the crack plane.

The role of S is purely geometric: it ensures the correct sign for each coordinate, so that nodes are placed in all four quadrants surrounding the crack tip.

*The four nodes of the crack front*

The second part of the study presents the crack propagation coordinates of the nodes, obtained by the CPCN-FEM Finite Element Method and explained using different equations based on the two axes (X and Y).

Consequently, for node 2900, we obtain equations (9) and (10) as follows:

$$X(2900) = a + \frac{\phi}{2}\left[\sum_{q=1}^{i-1} cos \sum_{j=1}^{q}(\beta_j)(-1)^i sin \sum_{j=1}^{i}(\beta_j)\right] \quad (9)$$

a is crack length, ϕ is crack front length and β is the angle of crack inclination.

$$Y(2900) = \frac{\phi}{2}\left[\sum_{q=1}^{i-1} sin \sum_{j=1}^{q}(\beta_j) + cos\left(\sum_{j=1}^{i}(\beta_j)\right)\right] \quad (10)$$

with i=1, ..,6.

Equations (11) and (12) describe the coordinates of node 2100.

$$X(2100) = a + \frac{\phi}{2}\left[\sum_{q=1}^{i-1} cos \sum_{j=1}^{q}(\beta_j)(-1)^i sin\left(\sum_{j=1}^{i}(\beta_j)\right) + cos\left(\sum_{j=1}^{i}(\beta_j)\right)\right] \quad (11)$$

with i=1, ..,6.

$$Y(2100) = \frac{\phi}{2}\left[cos \sum_{j=1}^{i}(\beta_j) + \sum_{q=1}^{i} sin \sum_{j=1}^{q}(\beta_j) + sin\left(\sum_{j=1}^{i}(\beta_j)\right)\right] \quad (12)$$

with i=1, ..,6.

Node 1300 is defined during crack propagation by the coordinate obtained by equations (13) and (14).

$$X(1300) = a + \frac{\phi}{2}\left[\sum_{q=1}^{i} cos \sum_{j=1}^{q}(\beta_j) + cos \sum_{j=1}^{i}(\beta_j) + sin \sum_{j=1}^{i}(\beta_j)\right] \quad (13)$$

with i=1, ..,6.

$$Y(1300) = \frac{\phi}{2}\left[\sum_{q=1}^{i} sin \sum_{j=1}^{q}(\beta_j) + sin \sum_{j=1}^{i}(\beta_j) - cos \sum_{j=1}^{i}(\beta_j)\right] \quad (14)$$

with i=1, ..,6.

For the different stages of crack propagation concerning node 500, we have the coordinates (15) and (16):

$$X(500) = a + \frac{\phi}{2}\left[\sum_{q=1}^{i} cos \sum_{j=1}^{q}(\beta_j) + sin \sum_{j=1}^{i}(\beta_j)\right] \quad (15)$$

with i=1, ..,6.

$$Y(500) = \frac{\phi}{2}\left[\sum_{q=1}^{i} sin \sum_{j=1}^{q}(\beta_j) - cos \sum_{j=1}^{i}(\beta_j)\right] \quad (16)$$

with i=1, ..,6.

## Results and discussion

### *Numerical validation and mesh convergence*

To ensure the robustness of the numerical results, a convergence study was carried out using different mesh densities around the crack front. Several refined meshes were tested, including configurations with:

- Coarse mesh: average element size ≈ 0.5 mm,
- Medium mesh: ≈ 0.2 mm,
- Fine mesh: ≈ 0.1 mm around the crack tip.

The stress intensity factor (SIF) $K_I$ was computed for each configuration. Results showed that the relative variation of $K_I$ was below 2% between the medium and fine meshes, indicating that the solution is mesh-independent at the chosen resolution.

In addition, the numerical results were validated against analytical solutions for initial crack cases. The CPCN-FEM results showed excellent agreement, with an average relative error below 5% in the linear elastic fracture mechanics (LEFM) regime.

Computation time remained acceptable (less than 1 min per propagation step) due to the localized refinement strategy and the use of FORTRAN routines for node updates without global remeshing. We show the different extents of the initial crack front, for the four nodes that form the crack front. The nodes are numbered using the FORTRAN program,

and the four nodes are plotted using equation (8) concerning the two coordinates (X and Y), for the different crack lengths a = 1, 2, 3, 3.5 mm.

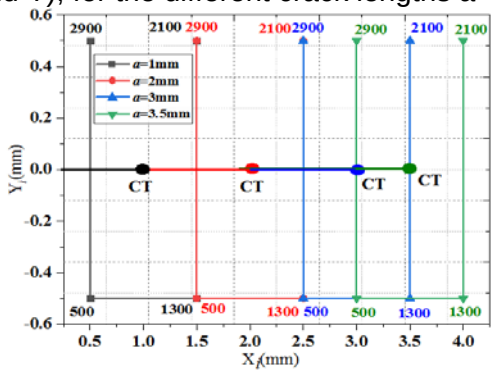


*Figure 8 - Node coordinates by CPCN-FEM method with i= 2900, 2100, 1300 and 500 regarding crack length a=1, 2, 3, and 3.5mm*

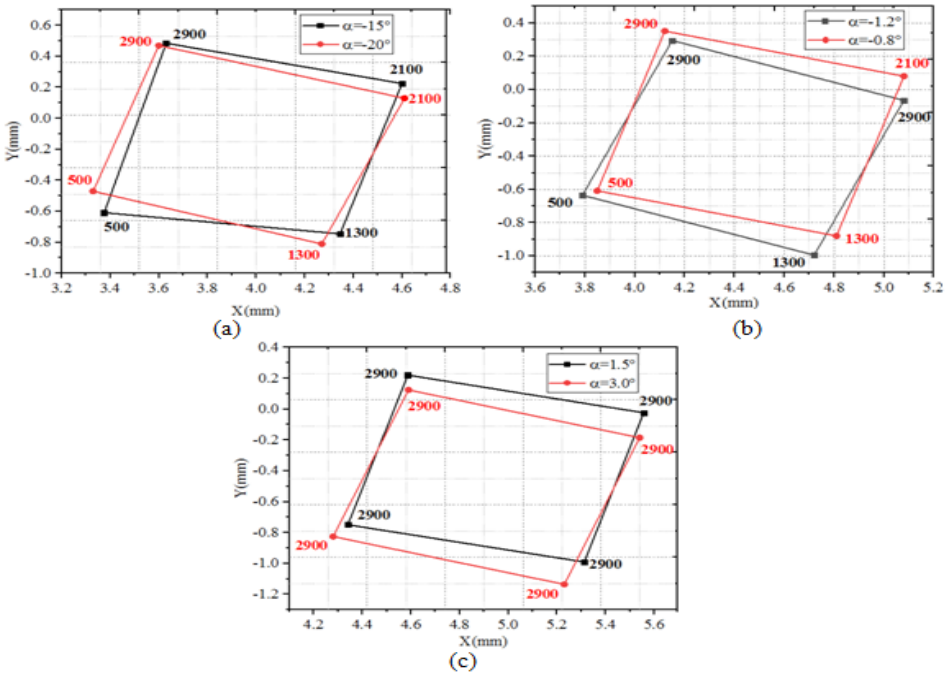


*Figure 9 - Variation of different crack front nodes for different crack angles: a) β=-15°, -20°; b) β=-1.2°, -0.8° and c) β=1.5°, 3.0°*

Figure 9 presents the variation of node positions in the X, Y plane, based on the application of equations (9) to (16) for different crack inclination angles: (a) β = –15° and –20°; (b) β = –1.2° and –0.8°; and (c)

β = 1.5° and 3.0°. Each configuration reveals that the nodes undergo a shift along both the X and Y axes, with the displacement interval in the X-direction depending significantly on the angle β. For instance, when β = –20°, the X-coordinate varies between approximately 3.33 mm and 4.61 mm, while for β = –15°, it ranges from 3.375 mm to 4.6 mm. These results indicate that as the crack propagates, the inclination angle tends to increase, influencing the deformation of the surrounding nodes. These variations can be attributed to the redistribution of stress fields around the crack tip, which becomes more anisotropic with increasing β. This anisotropy leads to directional displacement patterns in the material, especially in heterogeneous media, where crack paths are highly sensitive to local mechanical contrasts. Such behavior aligns with recent studies in fracture mechanics, which highlight that crack propagation often follows directions of maximum energy release or stress intensity (Worthington et al, 2023). The CPCN-FEM approach used here effectively captures these complex interactions between crack orientation and mechanical response, demonstrating its reliability for modeling advanced crack growth scenarios.

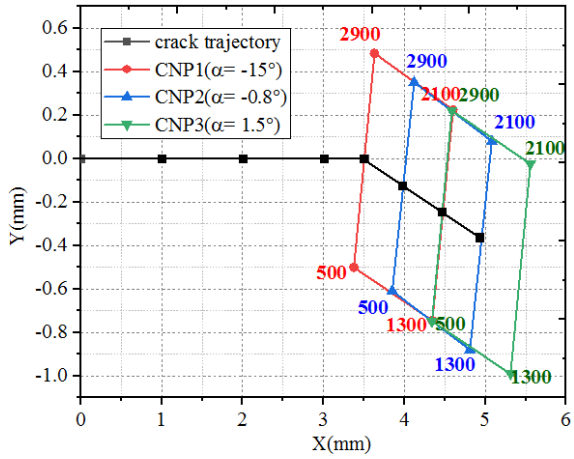


*Figure 10 - Comparison between three propagations by the CPCN-FEM method concerning the three angles: β=-15°, -0.8° and β=1.5°*

Figure 10 illustrates a comparison between three crack propagation scenarios, each inclined by a different angle: β = –15°, –0.8°, and 1.5°, as modeled using the CPCN-FEM approach. The crack trajectory, which extends up to a propagation length of a = 3.5 mm, is described by equation (8), while the propagation of each configuration is governed by equations (9) through (16). The figure clearly demonstrates that the CPCN-FEM method accurately captures the step-by-step evolution of the crack front

for various inclination angles without requiring any modification of the global mesh. This highlights one of the method's key advantages: the ability to model complex crack paths in a continuous domain with high precision. Physically, the observed differences in crack advancement for the three inclination angles can be attributed to the redistribution of local stress fields and the directional dependency of crack growth mechanisms. As the angle increases, the deviation of the crack front becomes more evident, reflecting the influence of anisotropy and the material's fracture resistance along different paths. These results are consistent with the findings of recent studies that emphasize the importance of incorporating orientation-dependent criteria in predictive fracture models (e.g., Guizhong et al, 2024). Overall, the CPCN-FEM method proves to be a robust and efficient tool for simulating realistic crack propagation without compromising mesh integrity.

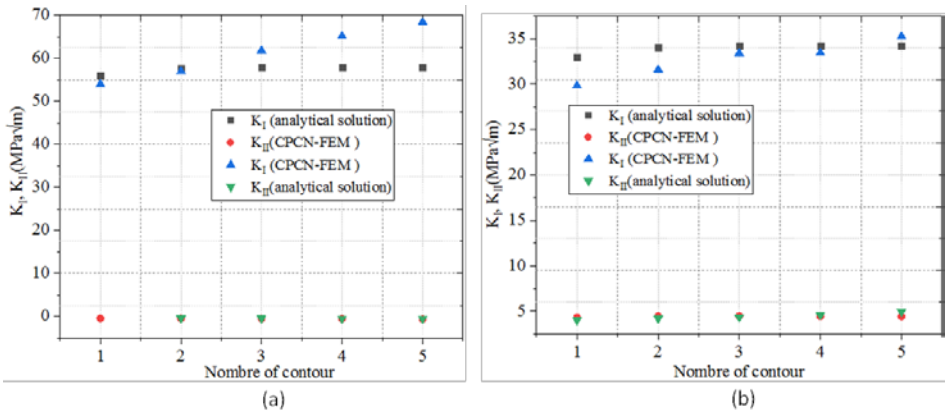


*Figure 11 - Evolution of stress intensity factors by the CPCN-FEM method: a) first propagation and b) second propagation*

Figure 11 illustrates the variation of the stress intensity factors $K_I$ and $K_{II}$ as a function of the number of contours, computed using the CPCN-FEM method. This analysis highlights the effectiveness of the numerical approach in accurately characterizing the stress field near the crack front.

In the first configuration (Figure 11a), which corresponds to a straight crack with an inclination angle $\beta = 0°$, $K_I$ increases gradually with the number of contours, while $K_{II}$ remains nearly constant and close to zero. This behavior indicates that the loading is predominantly Mode I, as expected for a straight crack subjected to symmetric conditions. The stability of $K_{II}$ suggests that the stress field is well-resolved and that the numerical formulation successfully isolates the mode components. The

strong agreement between the CPCN-FEM results and the analytical solution confirm the reliability of the method in modeling initial straight crack propagation.

Figure 11b presents the case of an inclined crack at β = 15°, which introduces a mixed-mode loading condition. Here, $K_I$ shows a similar trend to the previous case, increasing with the number of contours. However, $K_{II}$ remains constant at a non-negligible value, indicating the contribution of shear stresses due to the inclined crack front. Equations (8), (9), and (10) were used to simulate the crack extension along appropriate directions, accounting for the nodal positions along the crack front in both propagation scenarios.

These results demonstrate that increasing the number of contours improves the accuracy of $K_I$ estimation, while $K_{II}$, though sensitive to the crack orientation, remains relatively unaffected by this parameter. This observation is consistent with the findings of Keprate et al. (2019), who emphasized the role of contour selection and mesh refinement in the accurate evaluation of stress intensity factors. Furthermore, recent studies (Gdoutos et al., 2012; Fayed et al., 2017) have shown that combining mode decomposition techniques with multi-contour integration enhances the fidelity of numerical predictions, particularly in mixed-mode fracture problems involving anisotropic or composite materials.

The good agreement between the CPCN-FEM results and the analytical solutions across both cases reinforces the validity of the numerical method. The approach proves to be robust for simulating crack propagation in both straight and inclined configurations, accurately capturing the relative contributions of Modes I and II.

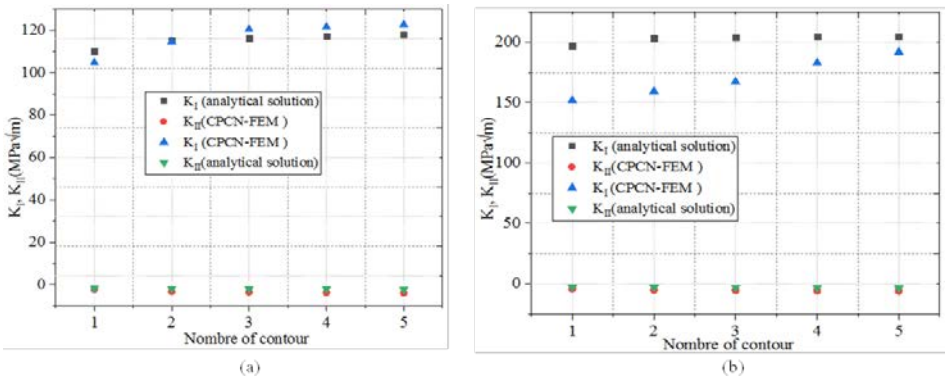


*Figure 12 - Evolution of stress intensity factors by the CPCN-FEM method; a) third propagation and b) fourth propagation*

Figure 12 shows the variation of the stress intensity factors $K_I$ and $K_{II}$ as a function of the number of contours for the third (Figure 12a) and fourth (Figure 12b) crack propagation scenarios, using the CPCN-FEM method. These cases correspond to more advanced stages of crack growth, where the geometry and the stress field become increasingly complex.

In the third propagation case (Figure 12a), the values of $K_I$ increase significantly with the number of contours, stabilizing around 120 MPa√m. This trend indicates a clear sensitivity of the stress intensity factor to the extent of crack growth. The increase in $K_I$is consistent with the physical expectation that a longer or more evolved crack experiences a higher stress concentration at its tip. Meanwhile, $K_{II}$ remains low and nearly constant, suggesting that Mode I still dominates and that the numerical approach is effective in capturing the crack tip singularity in this configuration.

In the fourth propagation case (Figure 12b), the values of $K_I$ are even higher, reaching up to approximately 200 MPa√m, which aligns with the progression of the crack and the corresponding increase in energy release rate. This rise in $K_I$ reflects the cumulative effect of crack length and propagation angle, both of which contribute to intensified stress conditions at the crack front. As in the previous case, $K_{II}$ remains stable across all contours, further confirming that the CPCN-FEM method reliably separates the contributions of each fracture mode.

These results support the theoretical understanding that the stress intensity factor $K_I$ increases with crack length and propagation, as confirmed in studies such as those by Fayed et al. (2017) and Kumar et al. (2016), which highlight the dependency of fracture parameters on crack geometry and material configuration. Furthermore, the consistent results across multiple contours reflect the robustness of the CPCN-FEM technique, especially in modeling cracks under complex, multi-stage propagation paths. This is in agreement with findings from recent numerical investigations (Chang et al, 2014), where multi-contour techniques significantly improved accuracy in evaluating mixed-mode fracture parameters.

Overall, the comparison with analytical solutions demonstrates that the CPCN-FEM method remains accurate and effective, even in advanced crack propagation cases involving large stress gradients. The results underline its potential for reliable use in structural integrity assessments and fracture mechanics simulations of complex geometries.

## Conclusion

In this study, a novel numerical approach, CPCN-FEM (Crack Propagation via Coordinates of Nodes - Finite Element Method), was developed and applied to simulate the progressive propagation of a crack in an elastic, isotropic material. The method centers on the strategic generation of four key nodes around the crack front to guide its directional growth at each propagation stage. This approach enabled accurate tracking of crack path geometry while maintaining a stable mesh configuration, thanks to the FORTRAN-based node-updating algorithm.

One of the major contributions of this work lies in the ability of CPCN-FEM to compute the stress intensity factors (SIFs) in Modes I and II ($K_I$ and $K_{II}$), as well as to estimate the crack inclination angle (β), with high consistency across multiple propagation stages. The method's validity was confirmed through comparative analysis with classical analytical solutions, showing excellent agreement in both crack trajectory and SIF values. Additionally, the study demonstrated that changes in the crack angle result in measurable and predictable variations in the positions of the key nodes, reflecting the sensitivity and robustness of the proposed model.

By avoiding the need for full remeshing during crack growth, CPCN-FEM offers a highly efficient solution suitable for large-scale simulations or real-time fracture analysis. Its simplicity in node control, combined with its compatibility with standard finite element frameworks, makes it an attractive tool for researchers and engineers working in fracture mechanics, fatigue analysis, and damage tolerance assessment.

Looking forward, this method can be further extended to account for nonlinear material behavior, anisotropic properties, and thermal or environmental effects. It also holds potential for integration with experimental crack tracking data, enabling hybrid approaches for validating simulation accuracy. Moreover, coupling the CPCN-FEM model with adaptive meshing strategies and 3D implementations would significantly enhance its applicability to more complex real-world structures and loading conditions.

In conclusion, the CPCN-FEM method provides a reliable, computationally efficient, and theoretically sound framework for analyzing crack propagation in 2D elastic structures, paving the way for future advancements in digital fracture mechanics.

## References


Abdulnaser Alshoaibi and Ahmad Kamal Ariffin. 2015. Finite Element Modeling of Fatigue Crack Propagation Using a Self Adaptive Mesh Strategy, *International Review of Aerospace Engineering (IREASE)*, 8(6):209, Available at: https://doi.org/10.15866/irease.v8i6.8823

AlshoaibI, A. M. and Fageehi, Y. A. 2023. A Computational Framework for 2D Crack Growth Based on the Adaptive Finite. Element Method, *Appl. Sci,* v. 13, n. 1, 2023. 284, https:// doi.org/10.3390/app13010284

Amestoy, M. Bui, H.D. and Dang Van K. 1980. [In:] *International Advances in Fracture Research,* Fran¸cois D. et al. (Eds.), Oxford, pp. 107-113.

Bentahar M. 2023. ALLDMD Dissipation Energy Analysis by the Method Extended Finite Elements of a 2D Cracked Structure of an Elastic Linear Isotropic Homogeneous Material. *Journal of Electronics, Computer Networking and Applied Mathematics,* v. 3, n. 2, pp. 1-8, 2023. Available at: https://doi.org/10.55529/jecnam.32.1.8

Bentahar, M. 2023. Fatigue Analysis of an Inclined Crack Propagation Problem by the X-FEM Method. *International Journal of Applied and Structural Mechanics (IJASM),* v. 3, n. 4, pp. 23–31, Available at: https://doi.org/10.55529/ijasm.34.23.31

Bentahar, M. Benzaama, H. and Mahmoudi, N. 2021. Numerical modeling of the evolution of the strain energy ALLSE of the crack propagation by the X-FEM method. *Revue des matériaux et énergies renouvelables*, v. 5, n. 2, pp. 24-31, Available at : https://asjp.cerist.dz/en/article/167392

Bilby, B. A., and Cardew, G. E. 1975. The crack with a kinked tip. *International Journal of Fracture,* 11, pp. 708-712. Available at: https://doi.org/10.1007/BF00116380

Borges, M. F. Lopez-Crespo, P. Antunes, F.V. Moreno, B. Prates, P. Camas, D. and Neto, D.M. 2021. Fatigue crack propagation analysis in 2024-T351 aluminium alloy using nonlinear parameters, *International Journal of Fatigue,* V153, 106478, Available at: https://doi.org/10.1016/j.ijfatigue.2021.106478.

Chang, J. H., & Jiang, J. Y. 2014. Modified Contour Integrals for Calculation of Stress Intensity Factors for Cracks in Anisotropic FGMs. *Applied Mechanics and Materials*, 627, 129-133. Available at: https://doi.org/10.4028/www.scientific.net/AMM.627.129

Crusat, L. Carol, I. and Garolera, D. 2021. Application of configurational mechanics to crack propagation in quasi-brittle materials*, Engineering Fracture Mechanics*, V 241, 107349, Available at: https://doi.org/10.1016/j.engfracmech.2020.107349

Elguedj, T. 2006. Simulation numérique de la propagation de fissure en fatigue par la méthode des éléments finis étendus : thèse prise en compte de la plasticité et du contact-frottement*, lamcos - umr cnrs* 5514 - INSA de Lyon 20, avenue Albert Einstein, 69621 Villeurbanne Cedex (FRANCE).

Erdogan, F. and Sih G.C. 1963. On the crack extension in plates under plane loading and shear, *Journal of Basic Engineering*, 85, 4, pp. 519-527. Available at: https://doi.org/10.1115/1.3656897

Fayed, A. S. 2017. Numerical analysis of mixed mode I/II stress intensity factors of edge slant cracked plates. *Engineering Solid Mechanics*, 5(1), 61-70. Available at: https://doi.org/10.5267/j.esm.2016.8.001

Gdoutos, E. E. 2012. Problems of mixed mode crack propagation (Vol. 2). *Springer Science & Business Media*.

Guizhong, X. I. E., Chongmao, Z. H. A. O., Hao, L. I., Jun, L. I. U., Wenliao, D. U., Jiahe, L. V., & Chao, W. U. 2024. An adaptive extended finite element based crack propagation analysis method. *Mechanics,* 30(1), 74-82. Available at: https://doi.org/10.5755/j02.mech.33301

Ilie, P. and Ince, A. 2022. Three-dimensional fatigue crack growth simulation and fatigue life assessment based on finite element analysis*, Fatigue & Fracture of Engineering Materials & Structures*, v.45, n.11, pp. 3251-3266, Available at: https://doi.org/10.1111/ffe.13815

Keprate, A., Chandima Ratnayake, R. M., & Sankararaman, S. 2019. Experimental validation of the adaptive Gaussian process regression model used for prediction of stress intensity factor as an alternative to finite element method. *Journal of Offshore Mechanics and Arctic Engineering*, 141(2), 021606. Available at: https://doi.org/10.1115/1.4041457

Kocańda, D. and Torzewski, J. 2009. Deterministic approach to predicting the fatigue crack growth in the 2024-t3 aluminum alloy under variable amplitude loading *, Fatigue of Aircraft Structures,* Vol. 1, pp.102-115, Available at: https://doi.org/10.2478/v10164-010-0010-1

Kumar, D., Roy, R., Kweon, J. H., & Choi, J. H. 2016. Numerical modeling of combined matrix cracking and delamination in composite laminates using cohesive elements. *Applied Composite Materials*, 23, 397-419. , Available at: doi.org/10.1007/s10443-015-9465-0

Mehmet, F. Yaren, M. F. Ayhan, A. O. 2024. A new method for prediction of fatigue crack propagation life under variable amplitude spectrum loading, *Theoretical and Applied Fracture Mechanics,* Volume 131, 104355, , Available at: https://doi.org/10.1016/j.tafmec.2024.104355

Montassir, S. Moustabchir, H. and Elkhalfi, A. 2023. Application of NURBS in the Fracture Mechanics Framework to Study the Stress Intensity Factor. Statistics, *Optimization and Information Computing*, v. 11, n. 1, pp. 106–115. Available at: https://doi.org/10.19139/soic-2310-5070-1553

Nie, Y. Wang, X. Wu, B. Zhang, G. Gamage, R. P. Li, Shiyuan. and Zhang, L. 2025. Influences of the stress ratio and local micro mineral aggregates on small fatigue crack propagation in the shale containing bedding planes, *International Journal of Rock Mechanics and Mining Sciences,* V185, 105980, Available at: https://doi.org/10.1016/j.ijrmms.2024.105980

Niu, Y. Fan, J. Shi, X. Wei, J. Jiao, C. and Hu, J. 2023. Application of the J-Integral and Digital Image Correlation (DIC) to Determination of Multiple Crack

Propagation Law of UHPC under Flexural Cyclic Loading. *Materials,* v. 6, p. 1296, Available at: https://doi.org/10.3390/ma16010296

Nuismer, R.J. 1975. An energy release rate criterion for mixed mode fracture*, International Journal of Fracture*, 11, 2, pp. 245-250. Available at: https://doi.org/10.1007/BF00038891

Pramana, N. et al. 2024.Experimental and numerical analysis of crack propagation material Al 2024 under spectrum load. *AIP Conference Proceedings.* Vol. 3003. No. 1. AIP Publishing LLC, Available at: https://doi.org/10.1063/5.0186423

Rahman, M. Maeda, T. Osada, T. and Ozaki, S. 2024. Finite element analysis of crack propagation, crack-gap-filling, and recovery behavior of mechanical properties in oxidation-induced self-healing ceramics*, International Journal of Solids and Structures*, v. 306, n.3, 113104, Available at: https://doi.org/10.1016/j.ijsolstr.2024.113104

Ricardo, L.C.H. 2018. Crack Propagation by Finite Element Method, *Frattura edIntegrità Strutturale*, v. 12, n. 43, pp. 57-78. , Available at: : https://doi.org/10.3221/IGF-ESIS.43.04

Richard, H. A. 2004. Fulland, M and Sander, M. Theoretical crack path prediction Publishing Ltd. *Fatigue Fract Engng Mater Struct* 28, pp. 3-12. Available at : https://doi.org/10.1111/j.1460-2695.2004.00855.x

Richard, H.A. 1985. Bruchvorhersagen bei überlagerter Normal- und Schubbeanspruchung von Rissen.*VDI-Forschungsheft* 631. VDI-Verlag, Düsseldorf. ISBN: 3188506317

Robles, J .M. Vasco-Olmo, J.M. Cruces, A.S. Diaz, F.A. James, M.N. and Lopez-Crespo, P. 2023. Fatigue crack characterisation in 2024-T351 aluminium alloy through SEM observation combined with the CJP model, *International Journal of Fatigue*Volume 166, 107279, Available at: https://doi.org/10.1016/j.ijfatigue.2022.107279

Sadek, M. Bergström, J. and Hallbäck, N. 2024. Computing the stress intensity factor range for fatigue crack growth testing at 20 kHz. *Engineering Reports*. 6(6):e12792. Available at: https://doi.org/10.1002/eng2.12792

Saverio, F. 2014. Modélisation tridimensionnelle de la fermeture induite par plasticité lors de la propagation d'une fissure de fatigue dans l'acier 304L. Thèse (Doctorat) – *L'Ecole Nationale Supérieure de Mécanique* et *D'Aérotechnique.* Soutenue le 24/11/2014. https://theses.hal.science/tel01129079

Sedmak, A. 2023. Fatigue crack growth simulation by extended finite element method: A review of case studies. Fatigue Fract. Eng. *Mater. Struct*. c, 47, pp. 1819–1855. Available at: https://doi.org/10.1111/ffe.14277

Sedmak, A. Grbović, A. Gubeljak, N. Sedmak, S. and Budimir, N. 2024 Numerical Simulation of Fatigue Crack Growth and Fracture in Welded Joints Using XFEM—A Review of Case Studies*. Materials* , 17, 5531. Available at: https://doi.org/10.3390/ma17225531

Si, Z. Yu, T. Fang, W. Natarajan, S. 2024. An adaptive multi-patch isogeometric phase-field model for fatigue fracture. *Int. J. Mech*. Sci.2024, 271, 109146. Available at: https://doi.org/10.1016/j.ijmecsci.2024.109146

Tada H.P., Paris P.C. and Irwin G.R. 2000. The Stress Analysis of Cracks Handbook, *American Society of Mechanical Engineering.* Available at: https://doi.org/10.1115/1.801535

Worthington, M., & Chew, H. B. 2023. Crack path predictions in heterogeneous media by machine learning. *Journal of the Mechanics and Physics of Solids,* 172, 105188. Available at : https://doi.org/10.1016/j.jmps.2022.105188

Wysmulski, P. 2023. Numerical and Experimental Study of Crack Propagation in the Tensile Composite Plate with the Open Hole , *Adv. Sci. Technol. Res. J.* v. 17, n.4, pp. 249-261, Available at: https://doi.org/10.12913/22998624/169970

Yaren, M. F. Ayhan, A. O. 2024. A new method for prediction of fatigue crack propagation life under variable amplitude spectrum loading, *Theoretical and Applied Fracture Mechanics*, Volume 131, 104355,Available at: https://doi.org/10.1016/j.tafmec.2024.104355

Zhang, T. Yu, T. Ding, J. and Natarajan, S. 2024. Low-cycle fatigue crack growth in brittle materials: Adaptive phase-field modeling withvariable-node elements*. Comput. Methods Appl. Mech*. Eng. 2024, 425, 116917.Available at : https://doi.org/10.1016/j.cma.2024.116917

Zhang, T. Yu, T. Li, Y. Bui, T.Q. 2023. Crack growth in anisotropic brittle and polycrystalline materials by adaptive phase field modelusing variable-node elements*. Finite Elem. Anal.* Des. 217, 103909. Available at : https://doi.org/10.1016/j.finel.2023.103909

Zienkiewicz, O.C. Taylor, R.L. and Zhu, J.Z. 2005.The Finite Element Method: Its Basis and Fundamentals*; Elsevier:* Amsterdam, The Netherlands. ISBN: 9780080472775

---

Modeliranje širenja pukotine zamora u 2D strukturama primenom CPCN-FEM pristupa koji se zasniva na čvorovima

*Mohammed* Bentahar[a], **autor za prepisku**, *Noureddine* Mahmoudi[a], *Nedir* Hachemi[b], *Youcef* Moulai Arbi[c]

[a] Universiy of Saida Dr. Moulay Tahar, Faculty of Technology, Department of Civil Engineering and Hydraulics, Saida, People's Democratic Republic of Algeria

[b] University of Mustapha Stambouli, Mascara,People's Democratic Republic of Algeria

[c] University of Mustapha Stambouli, Laboratory of Quantum Physics of Matter and Mathematical Modeling (LPQ3M), Mascara, People's Democratic Republic of Algeria

OBLAST: mašinstvo, materijali
KATEGORIJA (TIP) ČLANKA: originalni naučni rad

*Sažetak:*

*Uvod/cilj: Cilj ovog rada je modeliranje širenja pukotina nastalih usled zamora uvođenjem numeričke metode CPCN-FEM (eng. Crack Propagation by Coordinates of Nodes – Finite Element Method) koja predviđa putanje pukotina sistematskim generisanjem koordinata čvorova oko fronta pukotine.*

*Metode: Pristup definiše četiri glavna čvora za kontrolu pravca širenja i izračunava faktore intenziteta napona (K I) i (K II), kao i ugao nagiba pukotine (β). Metoda je implementirana u FORTRAN-u radi automatizacije praćenja čvorova, ažuriranja koordinata i postepenog napredovanja pukotine u dvodimenzionalnom elastičnom izotropnom modelu. Simulacije se sprovode i upoređuju sa analitičkim rešenjima putanje pukotine koristeći Ričardov kriterijum za određivanje orijentacije pukotine.*

*Rezultati: Numerički model je reprodukovao očekivane putanje pukotina uz visoko podudaranje sa analitičkim predviđanjima i pokazao stabilno ponašanje pomeranja kroz više slučajeva širenja. Integritet mreže je očuvan tokom svih koraka širenja.*

*Zaključak: Rezultati pokazuju da metoda CPCN-FEM predstavlja tačnu, efikasnu i mrežno stabilnu tehniku za modeliranje širenja pukotina nastalih usled zamora koja pruža pouzdana predviđanja evolucije putanje pukotine u mehanici loma.*

*Ključne reči: širenje pukotina, faktor intenziteta napona (SIF), metoda konačnih elemenata, CPCN-FEM, koordinate čvorova, mehanika loma.*

Paper received on: 4 June 2025.
Manuscript corrections submitted on: 28 November 2025.
Paper accepted for publishing on: 21 November 2025.